Combining Gradient and Albedo Data for Rotation Invariant Classification of 3D Surface Texture

Jiahua Wu
Silsoe Research Institute
Wrest Park
Silsoe
Beds
MK45 4HS
United Kingdom
jerry.wu@bbsrc.ac.uk

Mike J Chantler
Texture Lab
School of Mathematical and Computer Sciences
Heriot-Watt University
Edinburgh
EH14 4AS
United Kingdom
m.j.chantler@hw.ac.uk

Abstract

We present a new texture classification scheme which is invariant to surface-rotation. Many texture classification approaches have been presented in the past that are image-rotation invariant, However, image rotation is not necessarily the same as surface rotation. We have therefore developed a classifier that uses invariants that are derived from surface properties rather than image properties. Previously we developed a scheme that used surface gradient (normal) fields estimated using photometric stereo. In this paper we augment these data with albedo information and an also employ an additional feature set: the radial spectrum.

We used 30 real textures to test the new classifier. A classification accuracy of 91% was achieved when albedo and gradient 1D polar and radial features were combined. The best performance was also achieved by using 2D albedo and gradient spectra. The classification accuracy is 99%.

1. Introduction

Many texture classification schemes have been presented that are invariant to image rotation [1,2,3]. They normally derive their features directly from a single image and are tested using rotated images. However, in many cases rotation of a textured surface produces images that differ significantly from those provided by pure image rotation (see Fig. 1). Few take into account these problems. Exceptions include Leung and Malik's classification system which uses the images obtained under 20 different illumination and orientation conditions [8]; Nayer & Dana who developed histogram and correlation models of 3D surface textures by using CUReT database [16]; Dana *et al.* developed BTF (Bi-directional Texture Function) database which described the appearance of a textured surface as a function of the illumination and viewing directions [17], and McGunnigle and Chantler who proposed rotation insensitive scheme that uses photometric stereo to obtain gradient information [9,10]. In [15] we presented an approach that uses polarograms of surface gradient fields estimated using photometric stereo.

In this paper, we concern illumination effects due to frontal views. We augment the feature space in two ways. Firstly we use radial spectra in addition to the polarograms [6] (or polar spectra). Secondly we apply these feature generators to both albedo and gradient data.

We use photometric stereo to obtain the gradient and albedo information. They are Fourier transformed and combined to provide a frequency domain function that does not contain the directional artifacts associated with partial derivatives. Polar and radial spectra of these data are compared with those of training classes. Radial spectra are rotation insensitive and therefore comparison is performed using a simple sum of squared differences metric. Polar spectra are rotation sensitive - a rotation of the surface corresponds to a translation of its polar spectrum. Thus a test texture's polar spectrum must be translated through *180°* to find the best match for each class. This provides an estimate of the orientation of the test texture as well as the comparison metric.

Proceedings of the Ninth IEEE International Conference on Computer Vision (ICCV 2003) 2-Volume Set
0-7695-1950-4/03 $17.00 © 2003 IEEE

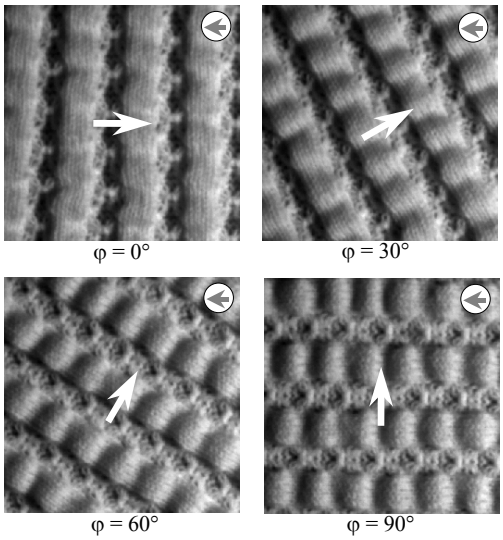

Fig. 1 - Four images of the same directional 3D rotated surface texture with the constant illuminant. The surface has been rotated at angles of 0°, 30°, 60°, and 90° (indicated by the white arrows). The illuminant tilt was kept constant at τ = 0° (indicated by the black arrows in white circles).

2. The Components of the Classification Scheme

This section briefly describes the photometric algorithm, the process that we use to remove the directional artefacts from the partial derivatives, and provides definitions of the radial and polar spectra.

2.1. Photometric stereo

We assume a Lambertain reflectance function. This can be expressed in terms the partial derivatives of the surface height function:

$$i(x,y) = \rho(x,y)\left(\frac{-p(x,y)\cos\tau\sin\sigma - q(x,y)\sin\tau\sin\sigma + \cos\sigma}{\sqrt{p^2(x,y)+q^2(x,y)+1}}\right) \quad (1)$$

where: σ, τ are the illuminant's slant and tilt angles, $\rho(x,y)$ is the albedo of the surface, and the partial derivatives are as defined below:

$$p(x,y) = \partial z/\partial x \quad (2)$$

$$q(x,y) = \partial z/\partial y \quad (3)$$

Three images of the surface are taken under three different illumination conditions to provide three instances of eqn. 1. They are used at each (x,y) to solve for the three unknowns $\rho(x,y)$, $p(x,y)$, and $q(x,y)$ [10, 13, 14]. Fig. 2 shows an example of this process.

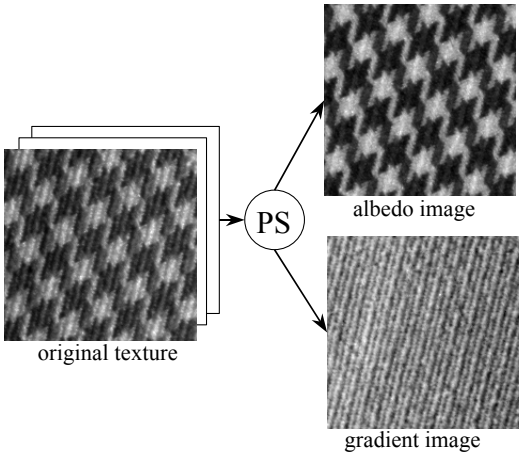

Fig. 2 - Extracting gradient and albedo data from 3D surface texture using photometric stereo. The gradient image was obtained by applying Lambertian rendering to the gradient fields p(x, y), and q(x, y).

An approximation to the albedo image could be obtained more simply using flat overhead illumination, however, we would still require two additional images for the calculation of the gradient data.

2.2. Deriving gradient and albedo spectra

We use frequency domain features and so the gradient and albedo data must be Fourier transformed. Transforming equations (2) and (3) gives:

$$P(u,v) = iuS(u,v) = i\omega\cos\theta\, S(\omega,\theta) \quad (4)$$

$$Q(u,v) = ivS(u,v) = i\omega\sin\theta\, S(\omega,\theta) \quad (5)$$

where: $S(u,v)$ and $S(\omega,\theta)$ are the surface magnitude spectrum in its Cartesian and polar forms, u, v are spatial frequency variables, and ω, θ are their polar equivalents.

Equations (4) and (5) show that both derivatives act as directional filters due to the $\cos\theta$ and $\sin\theta$ terms and can not therefore be used directly in a rotation invariant scheme. However, we may combine them to provide a gradient spectrum that is free of directional artifacts:

$$M(\omega,\theta) = |P(u,v)|^2 + |Q(u,v)|^2 = [\ \omega|S(u,v)|\ ]^2 \quad (6)$$

From Fig. 3, which shows the $M(\omega,\theta)$ gradient spectra of a selection of real textures, it can be seen that rotation

of each of the surfaces (from *30°* to *90°*) produces a corresponding rotation of their gradient spectra $M(\omega,\theta)$.

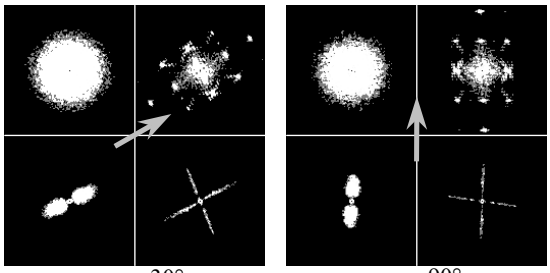

Fig. 3 - M(ω,θ) gradient spectra of real textures shown in montage format for two surface rotations (φ = 30° and 90°). The textures are gr2(left top), an4(right top), wv2(left bottom) and grd1(right bottom).

The albedo function $\rho(x, y)$ does not suffer from the same directional artifacts as the partial derivatives and may therefore be directly transformed and used:

$$A(\omega,\theta) = F[\rho(x, y)] \quad (7)$$

2.3. Polar and radial spectra

For classification we need to match the spectra of test and training textures in a rotation invariant manner. Comparing the gradient and albedo spectra of a test texture with those of the training classes over a complete range of rotations is computationally prohibitive. We therefore use two functions to compress the data but maintain their major characteristics: the polar and radial spectra.

We define the radial spectrum of the gradient data as:

$$\Phi_\alpha(\omega) = \int_0^{2\pi} M(\omega,\theta)\, d\theta \quad (8)$$

It summarizes the frequency content of the texture and is rotation insensitive as is shown in Fig. 4.

In contrast the polar spectrum summarises the directional characteristics of the surface:

$$\Pi_\alpha(\theta) = \int_0^{\infty} M(\omega,\theta)\, d\omega \quad (9)$$

This spectrum is a function of surface rotation; if the surface is rotated by an angle φ then a polar spectrum $\Pi_\varphi(\theta)$ will be produced, such that:

$$\Pi_\varphi(\theta) = \Pi(\theta+\varphi) \quad (10)$$

Gradient polar spectra of texture *wv2* are shown in Fig. 5. They confirm that a rotated texture's polar spectrum is approximately a translation of the non-rotated texture's polar spectrum.

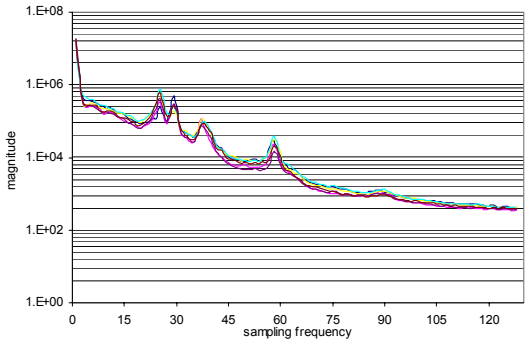

Fig. 4 - Radial gradient spectrum an4 at surface rotations of φ = 0°, 30°, 60°, 90°, 120° and 150°.

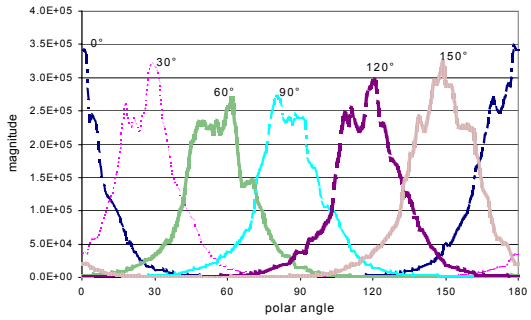

Fig. 5 - Polar spectra of wv2 at surface rotations of φ = 0°, 30°, 60°, 90°, 120° and 150°.

Thus we must compare polar spectra over a range angular displacements (φ_{test} = *0°, 1°, 2°, ..., 180°*) in order to determine the degree of correspondence and the relative angle of two surfaces.

Polar and radial spectra of albedo data $\rho(x, y)$ are also used in the classifier. These are used in a similar manner to the gradient spectra and are defined below:

$$\Phi_\beta(\omega) = \int_0^{2\pi} A(\omega,\theta)\, d\theta \quad (11)$$

$$\Pi_\beta(\theta) = \int_0^{\infty} A(\omega,\theta)\, d\omega \quad (12)$$

3. The Complete Classification Scheme

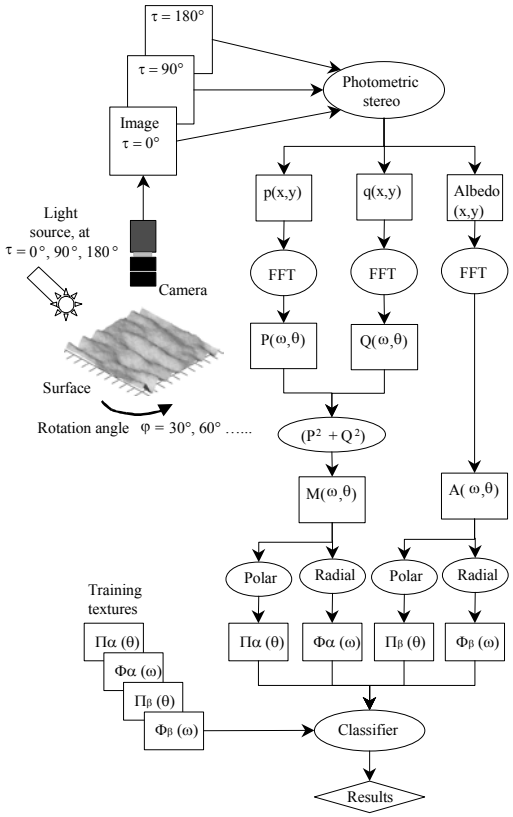

Fig. 6 - The surface rotation invariant classification scheme

The complete classification scheme is shown in Fig. 6. The process is as follows:

1. A photometric image set of the texture to be classified is captured (i.e. three images are taken at illuminant tilt angles of *0°*, *90°* and *180°*).
2. The photometric algorithm uses this image set to estimate the partial derivative and albedo fields: $p(x,y)$, $q(x,y)$ and $\rho(x,y)$.
3. These are Fourier transformed and processed to provide albedo and gradient polar and radial spectra.
4. The polar spectra are compared with polar spectra obtained from training images over a range of angular displacements (φ_{test}) using a sum of squared differences metric.
5. The radial spectra are compared with radial spectra obtained from training images. This also uses a sum of squared differences metric but it does not need to be calculated over a range of angular displacements.
6. The total sum of squared errors statistic is calculated from steps 4 and 5 and the best combination provides a classification decision and an estimate of the relative orientation of the test texture.

4. Results of Experiments

Experiments were performed using *30* real textures (Appendix A). A selection of the results is shown here which illustrate the nature of the features and the performance of the classifier.

4.1. Feature characteristics

Fig. 4 shows that radial spectra are insensitive to surface rotation while Fig. 5 shows that polar spectra undergo a translation as proposed previously.

Fig. 7 and Fig. 8 show that both radial and polar spectra contain useful discriminatory information.

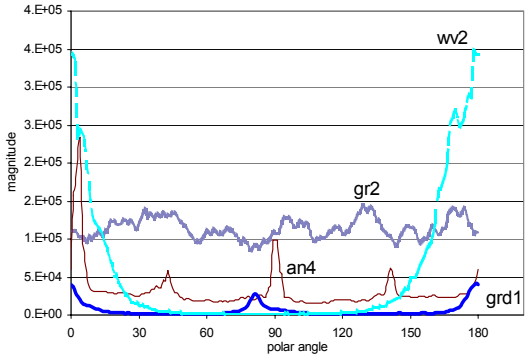

Fig. 7 - Polar plots of selective 4 real textures (an4, gr2, grd1 and wv2) on M(ω,θ) at surface rotation of φ = 0°.

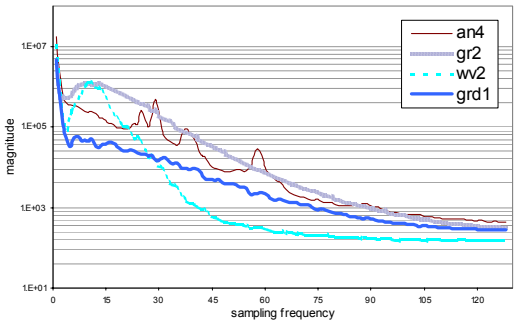

Fig. 8 - Radial plots of selective 4 real textures (an4, gr2, grd1 and wv2) on M(ω,θ) at surface rotation of φ = 0°.

4.2. Classification results

The classifier was trained using photometric image sets (512×512) from *30* surfaces obtained at a surface rotation angle of $\varphi = 0°$. This provided the 'training' radial and polar spectra.

Classification data was obtained from photometric image sets of the 30 texture samples obtained over a variety of surface rotation angles (*30°* to *180°* in *30°* increments). Each of the photometric sets was divided into nine smaller photometric sets each comprising three 256×256 images. This gave a total of 1620 (6×9×30) photometric test samples. Each of these test samples provided four spectra (gradient radial, gradient polar, albedo radial and albedo polar).

Fig. 9 shows the classification results per texture for three versions of the classifier by using polar and radial spectra. The "albedo" classifier used only the albedo radial and polar spectra to achieve a classification accuracy of *77%*, using gradient only data ("gradient") improved this figure to *86%*, while combining gradient and albedo data pushed the classification rate up to *91%*. It also shows that integration of the feature generators of gradient and albedo together provides more discriminative ability and comprehensive information for the classifier.

While these results are not quite as high as those published for some image rotation invariant schemes they are good considering the difficulties involved in rotation of real surface textures. In order to justify the cost and problems caused by photometric stereo imaging, such as shadow presented on texture *"rkb1"*, a comparison to the-state-of-art single image based methods will be done in future work.

4.3. Improved classification results by using 2D spectra

Why did misclassification happen? One reason is that the classification algorithm stops too soon. Step 6 in classification scheme compares 1D spectra only, however, these 1D spectra (polar and radial) are integrals of the original 2D spectra (gradient or albedo). Two textures with different 2D spectra may well have the same 1D spectra. Therefore a final verification step should be included where the 2D spectra are compared. This 2D comparison would not be costly because the rotation angles are already known from their 1D polar spectra. The complete classification scheme is shown in Fig. 10.

Fig. 11 shows the classification results per texture for three versions of the classifier by using 2D spectra. The classification accuracy of *95%* was achieved by using 2D gradient spectra only, and *93%* was achieved by using 2D albedo spectra only. The best performance was also improved by combining 2D gradient and albedo spectra. The classification accuracy is *99%*, a better result than that was presented in Fig. 9 by using 1D spectra.

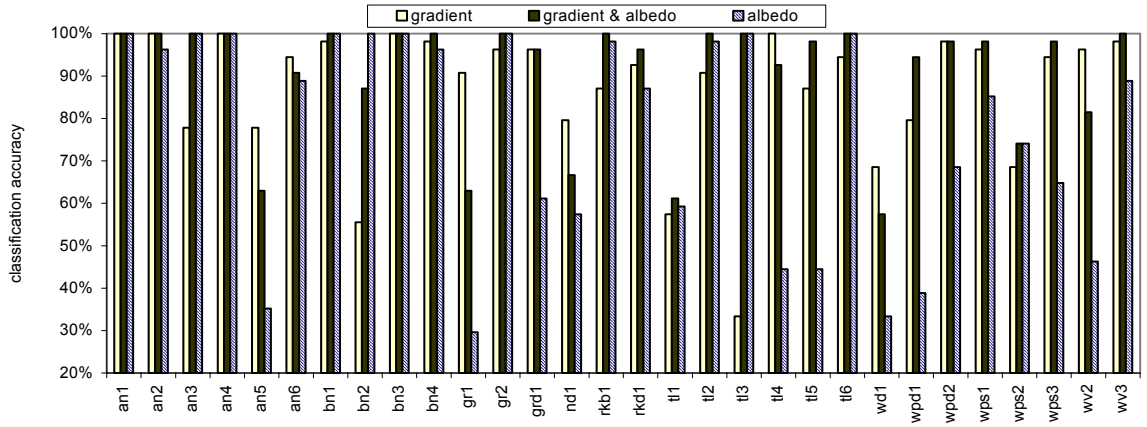

Fig. 9 - Classification results for 30 real textures by using *1D* polar and radial spectra.

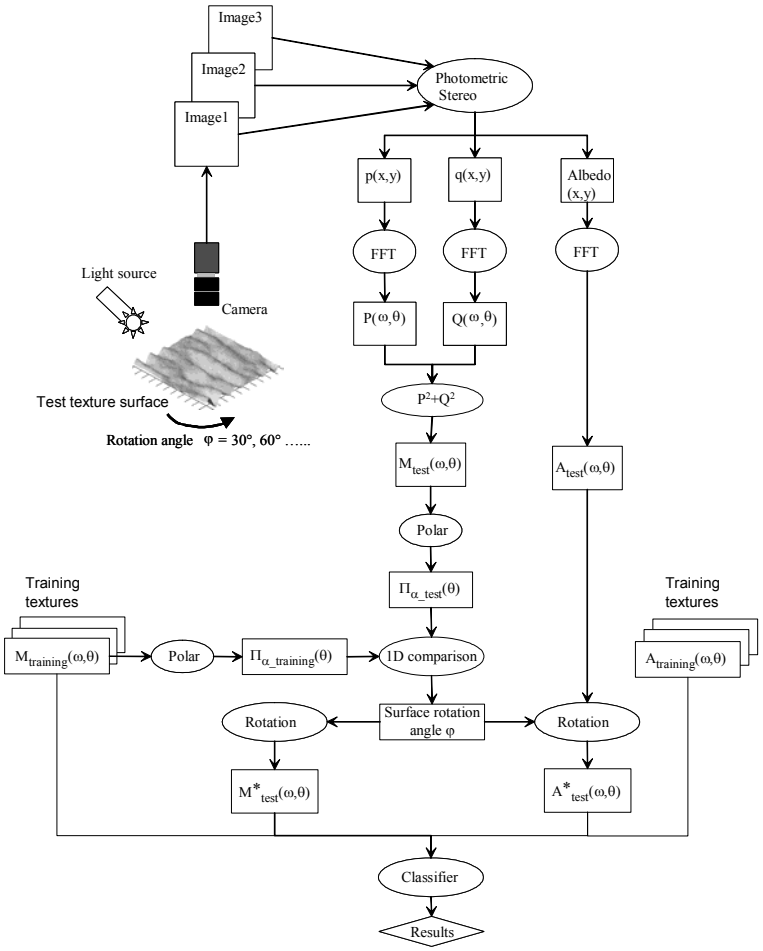

Fig. 10 – Surface rotation invariant classification scheme using *2D* spectra comparison.

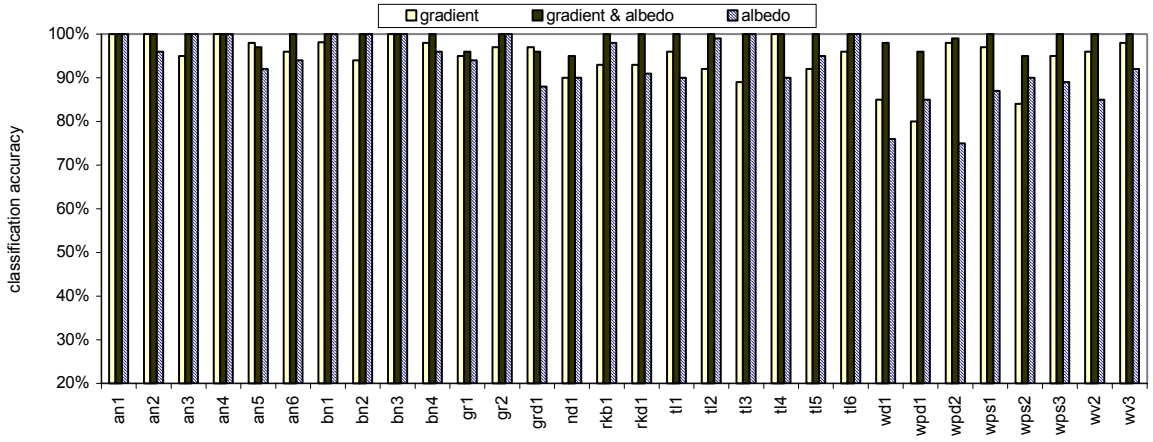

Fig. 11 – Classification results for 30 real textures by using *2D* spectra.

5. Conclusions

1. We have presented a new surface rotation invariant texture classification scheme that combines radial and polar spectra of albedo and gradient data.
2. We have presented theory and experimental results that show that the basic feature sets of radial and polar spectra of gradient and albedo data are free of directional artifacts.
3. Our results using *30* real textures show that combining albedo and gradient data improves the classification's performance to provide a successful classification rate of *99%.*

References

[1]. R. Porter & N. Canagarajah, "Robust rotation invariant texture classification: Wavelet, Gabor filter and GMRF based schemes", *IEE Proc. Vis. Image Signal Process,* Vol.144, No.3, June 1997.

[2]. F.S. Cohen, Z. Fan & M.A.S. Patel, "Classification of rotated and scaled textured images using Gaussian Markov field models", *PAMI* V13, February 1991, pp192-202

[3]. J. Mao & A.K. Jain, "Texture classification and segmentation using multiresolution simultaneous autoregressive models", *Pattern recognition*, V25, No.2, 1992, pp 173-188

[4]. M.J. Chantler, "The effect of illuminant direction on texture classification", *PhD Thesis*, Dept. of Computing and Electrical Engineering, Heriot-Watt University, 1994.

[5]. M.J. Chantler, G.T. Russell, L.M. Linnett "Illumination: A directional filter of texture?", *British Machine Vision Conference* 1994 Vol.2 pp.449-458.

[6]. L.S. Davis, "Polarograms: a new tool for image texture analysis", *Pattern Recognition*, V13, No. 3, 1981, pp219-223.

[7]. P. Brodatz, "*Textures: a photographic album for artists and designers*", Dover, New York, 1966.

[8]. T. Leung and J. Malik, "Recognizing Surfaces using Three-Dimensional Textons", *IEEE International Conference on Computer Vision*, Corfu, Greece, Sep 1999.

[9]. G. McGunningle, M.J. Chantler, "A model-based technique for the classification of textured surfaces with illuminant direction invariance", *Proceedings of BMVC97*, Essex, October 1997, pp470- 479.

[10]. G. McGunnigle, "The classification of textured surfaces under varying illuminant direction", *PhD Thesis*, Dept. of Computing and Electrical Engineering, Heriot-Watt University, 1998.

[11]. M. L. Smith, "The analysis of surface texture using photometric stereo acquisition and gradient space domain mapping", *Image and Vision Computing Journal*, Vol.17, 1009-1019, 1999.

[12]. G. McGunnigle & M.J. Chantler, "Rough surface classification using point statistics from photometric stereo", *Pattern Recognition Letters*, Vol.21, No.6-7, 2000, pp593-604.

[13]. G. Kay and T. Caelli, "Estimating the Parameters of an Illumination Model Using Photometric Stereo", *Graphical Models and Image Processing*, Vol.57, No.5 Sept. 1995, pp.365-388.

[14]. R. Woodham, "Photometric method for determining surface orientation from multiple images", *Optical Engineering*, Jan./Feb. 1980, Vol.19 No.1, pp.139-144.

[15]. M. J. Chantler & J. Wu, "Rotation Invariant Classification of 3D Surface Textures using Photometric Stereo and Surface Magnitude Spectra", *Proceedings of British Machine Vision Conference 2000*, Vol.2, pp486-495.

[16]. K. J. Dana and S. K. Nayar, "Correlation model for 3D texture", *Proc. of IEEE International Conference on Computer Vision*, Corfu, Greece, September 1999.

[17]. K. J. Dana, B. Van Ginneken, S. K. Nayar and J. J. Koenderink, "Reflectance and texture of real-world surfaces", *IEEE Conference on Computer Vision and Pattern Recognition*, pp.151-157, 1997.

APPENDIX A. 30 samples in our photometric texture database

(http://www.cee.hw.ac.uk/texturelab/database)

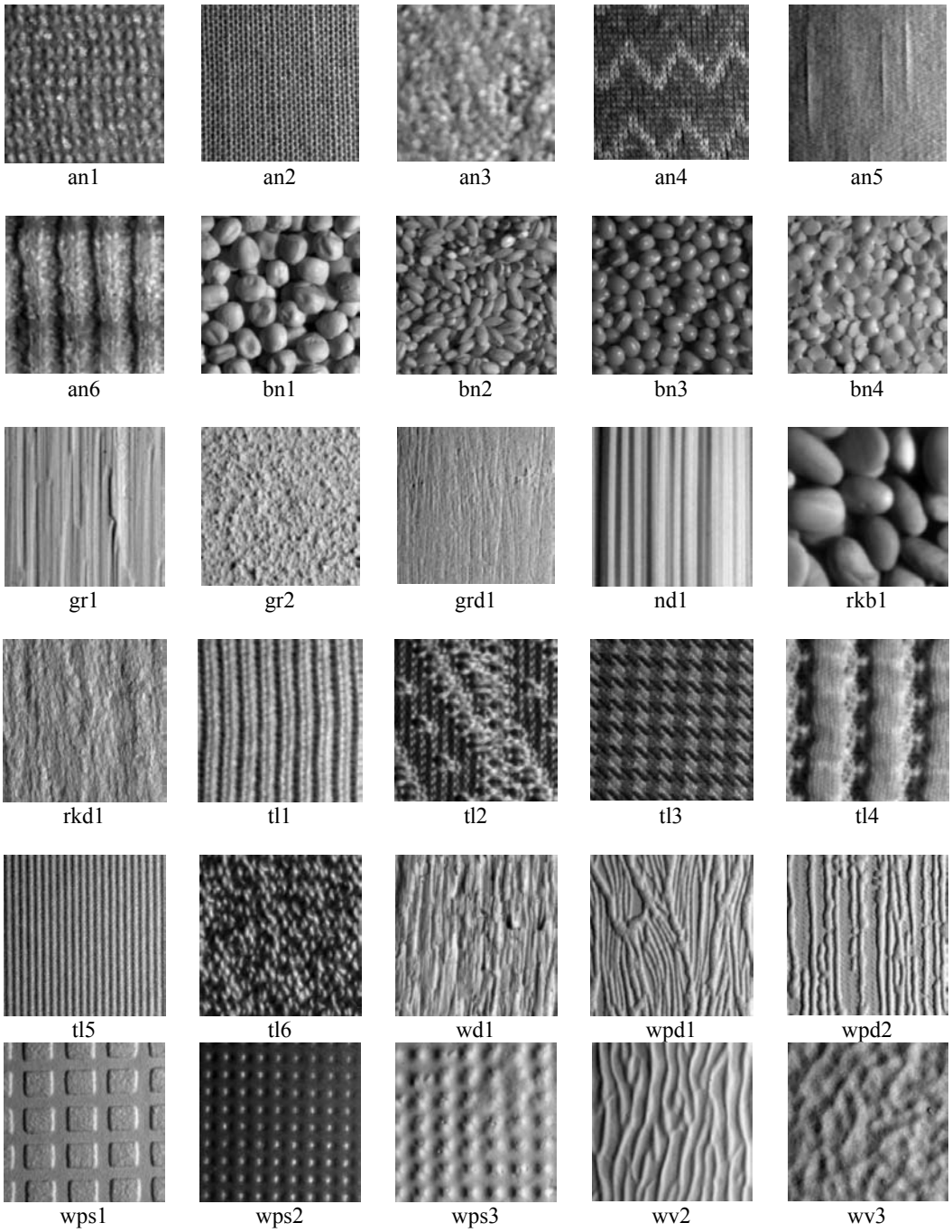

Proceedings of the Ninth IEEE International Conference on Computer Vision (ICCV 2003) 2-Volume Set
0-7695-1950-4/03 $17.00 © 2003 IEEE